Universität Potsdam

Christine Böckmann, Janos Sarközi

The ill-posed inversion of multiwavelength lidar data by a hybrid method of variable projection

NLD Preprints ; 53

The Ill-posed Inversion of Multiwavelength Lidar Data by a Hybrid Method of Variable Projection

Ch. Böckmann[a] and J. Sarközi[a]

[a]University of Potsdam, Institut of Mathematics, Postfach 601553
Potsdam D-14415 Germany

ABSTRACT

The ill-posed problem of aerosol distribution determination from a small number of backscatter and extinction lidar measurements was solved successfully via a hybrid method by a variable dimension of projection with B-Splines. Numerical simulation results with noisy data at different measurement situations show that it is possible to derive a reconstruction of the aerosol distribution only with 4 measurements.

Keywords: Ill-posed problem, inversion, variable projection method, multiwavelength Lidar, aerosol distribution

1. INTRODUCTION

Aerosol particle properties, which are needed to describe the influence of particles on the Earth's radiation budget, on clouds and precipitation, or their role in chemical processes of the troposphere and stratosphere, may be derived from measuring a certain variety of aerosol scattering properties. This can include extinction or scattering information at multiple wavelengths, scattering information at multiple angles, or multiple-scattering information. Here we discuss the inversion of particle properties from lidar measurements of backscattering and extinction at multiple wavelengths. At the Institute for Tropospheric Research Leipzig (IfT) a multiwavelength lidar has been developed which is capable of measuring the particle backscatter coefficient at six wavelengths and the particle extinction coefficient at two wavelengths. With these eight optical data or less up to four data the inversion is performed. The inversion requires the solution of a Fredholm integral equation system of the first kind which is an ill-posed problem.
At the Institute of Mathematics a hybrid method of variable projection for such an ill-posed inversion has been developed. After describing the mathematical model in Section 2, the mathematical background of the inversion is discussed in Section 3 followed by the theory of projection method as regularization tool in Section 4. In Section 5 we proposed our developed hybrid regularization method. Moreover, in Section 6 on the one hand side we show inversion results for simulated data to find a suitable B-Spline basis and on the other hand side we study a couple of real measurement situations with simulated and noisy data. An outlook of the influence of the unknown refractive index is given in Section 7.

2. MATHEMATICAL MODEL

The mathematical model for a LIDAR measurement consists of two linear Fredholm integral equations of the first kind for the backscatter and extinction coefficients β^{Aer} and α^{Aer}

$$\beta^{Aer}(\lambda,z) \;=\; \int_{r_{min}}^{r_{max}} k_\pi(r,\lambda;m)\; n(r,z)\; dr \;=\; \int_{r_{min}}^{r_{max}} \pi\; r^2\; Q_\pi(r,\lambda;m)\; n(r,z)\; dr\;, \tag{1}$$

$$\alpha^{Aer}(\lambda,z) \;=\; \int_{r_{min}}^{r_{max}} k_{ext}(r,\lambda;m)\; n(r,z)\; dr \;=\; \int_{r_{min}}^{r_{max}} \pi\; r^2\; Q_{ext}(r,\lambda;m)\; n(r,z)\; dr\;, \tag{2}$$

where r is the particle radius, m the refractive index, r_{min} and r_{max} are represent suitable lower and upper bounds of realistic radii, λ is the wavelength, z the height, n the aerosol size distribution we are looking for, k_π the backscatter

Other author information: (Send correspondence to Ch.B.)
Ch. B.: Email: bockmann@rz.uni-potsdam.de; WWW: http://math.uni-potsdam.de/~bockmann; Telephone: ++49-331-977-1743; Fax: ++49-331-977-1578; Supported by the BMBF under grant 07AF310/2.

and k_{ext} the extinction kernel. The backscatter coefficients are determined from backscattered signals and the extinction coefficients are determined from Raman signals, see Ansmann, Wandinger, Riebesell, Weitkamp, Michaelis.[1] The kernel function reflects shape, size and material composition of particles. We assume Mie-particles. The following formulas hold for extinction and backscatter efficiencies, see Bohren and Huffman,[2]

$$Q_\pi = \frac{1}{k^2r^2}|\sum_{n=1}^{\infty}(2n+1)(-1)^n(a_n - b_n)|^2, \quad Q_{ext} = \frac{2}{k^2r^2}\sum_{n=1}^{\infty}(2n+1)Re(a_n + b_n), \tag{3}$$

where k is the wave number defined by $k = 2\pi/\lambda$ and a_n and b_n are the coefficients which we get from the boundary conditions for the tangential components of the waves. The determination of the aerosol size distribution function $n(r)$ from a small number of backscatter and extinction measurements is an inverse ill-posed problem. Such problems may be interpreted as finding the cause of a given effect. Inverse problems of determination of system parameters from input-output measurements are often ill-posed in the sense that distinct causes can account for the same effect and small changes in a perceived effect can correspond to very large changes in a given cause.

3. MATHEMATICAL THEORETICAL BACKROUND

3.1. Compact Operators

We consider an equation of the form $Kx = y$ where $K : H_1 \to H_2$ is a compact, linear (but not necessarily self-adjoint) operator from a Hilbert space H_1 into a Hilbert space H_2. Firstly, we introduce some notations and definitions for linear operators in Hilbert spaces and refer to Groetsch.[3] A linear operator $K : H_1 \to H_2$ is called compact if $\overline{K(B)}$ is compact for each (norm) bounded subset B of H_1. The general theory of compact operators evolved from the theory of integral operators of the form

$$y(\lambda) = \int_{r_{min}}^{r_{max}} k(\lambda, r)\, x(r)\, dr \ . \tag{4}$$

Indeed, if $k(\cdot,\cdot)$ is square integrable over $[\lambda_{min}, \lambda_{max}] \times [r_{min}, r_{max}]$, then it is a well known classical result that K is a compact operator from $L^2[r_{min}, r_{max}]$ into $L^2[\lambda_{min}, \lambda_{max}]$. In addition, if $k(\cdot,\cdot)$ is continuous then K is a compact operator from $C[r_{min}, r_{max}]$ into $C[\lambda_{min}, \lambda_{max}]$ and from $L^2[r_{min}, r_{max}]$ into $L^2[\lambda_{min}, \lambda_{max}]$, respectively. A compact operator is continuous; in fact compact operators in Hilbert spaces may be characterized as linear operators which map weakly convergent sequences into strongly convergent sequences and hence compact operators are called completely continuous. It follows that a compact operator on a Hilbert space H is also compact on any Hilbert space which is continuously imbedded in H. In particular, the integral operator generated by a square integrable kernel is also compact when considered as an operator on the Sobolev spaces H_2^n.
The operators $K^*K : H_1 \to H_1$ and $KK^* : H_2 \to H_2$ are compact self-adjoint linear operators where K^* is the adjoint operator of K. The nonzero eigenvalues of K^*K or of KK^*, they have the same eigenvalues, can be enumerated as $\lambda_1 \geq \lambda_2 \geq \ldots$. If we designate by $v_1, v_2, \ldots$, an associated sequence of orthonormal eigenvectors of K^*K, then $\{v_1, v_2, \ldots\}$ is complete in the range $\overline{R(K^*K)} = N(K)^\perp$ (orthogonal compliment of the null space of K). Let $\mu_j = \sqrt{\lambda_j}$ then $Kv_j = \mu_j u_j$ and $K^*u_j = \mu_j v_j$. Moreover, $KK^*u_j = \mu_j Kv_j = \mu_j^2 u_j = \lambda_j u_j$ and it is not hard to see that the orthonormal eigenvectors $\{u_j\}$ of KK^* form a complete orthogonal set for $\overline{R(KK^*)} = N(K^*)^\perp$. The system $\{v_j, u_j; \mu_j\}$ is called a singular system for K and the numbers μ_j are called singular values of K. The next result is known as Picard's theorem on the existence of solutions of first kind equations. Let $K : H_1 \to H_2$ be a compact linear operator with singular system $\{v_j, u_j; \mu_j\}$. In order that the equation $Kx = y$ has a solution, it is necessary and sufficient that

$$y \in \overline{R(K)} = N(K^*)^\perp \quad \text{and} \quad \sum_{j=1}^{\infty} \lambda_j^{-1}|(y, u_j)|^2 < \infty.$$

The first condition may be viewed as an abstract smoothness or regularity condition in the sense that y inherits some of the smoothness (with respect to the first variable) of the kernel. Picard's theorem reinterprets this regularity by requiring that the components $|(y, u_j)|$ decay quickly relative to the growth of the singular values (recall that

$\lambda_j^{-1} \rightarrow \infty$ for nondegenerate kernels). Any $x \in H_1$ has a representation $x = Px + \sum_{j=1}^{\infty} < x, v_j > v_j$ where P is the orthogonal projector of H_1 onto $N(K)$ and hence

$$K\ x \ = \ \sum_{j=1}^{\infty} \mu_j \ < x, v_j > \ u_j \tag{5}$$

is the so called singular value decomposition of K. Any function of the form

$$x \ = \ \sum_{j=1}^{\infty} \frac{< y, u_j >}{\mu_j} \ v_j \ + \ \varphi \ \text{ where } \ \varphi \in N(K) \ \text{ is a solution.} \tag{6}$$

3.2. Ill-posed Problems

A Fredholm integral equation of the first kind is the most familiar and common example not only for a compact operator but also for a linear inverse ill-posed problem. Such equations are ill-posed on all three counts (existence, uniqueness and stability), where stability means a solution that changes only slightly with a slight change in the problem. We point out that instability is a hallmark of such equations. Very small changes in the right hand side $y(\lambda)$ can be accounted for by large changes in the solution $x(r)$. That the instability is fundamental, and not just a consequence of some special form of the kernels, follows from the Riemann-Lebesgue lemma. This means we have to look for a suitable regularization method. For a bounded linear operator K a solution only exists if and only if $y \in R(K)$. Since K is linear, $R(K)$ is a subspace of H_2, however, it generally does not exhaust H_2. We may enlarge the class of functions y for which a type of generalized solution exists to a dense subspace of function in H_2. This accomplished by introducing the idea of a least squares solution. A function $x \in H_1$ is called a least squares solution if

$$||Kx \ - \ y|| \ = \ \inf\{||Ku \ - \ y|| \ : \ u \in H_1\} \ . \tag{7}$$

This is equivalent to saying that $Py \in R(K)$, where P is the orthogonal projector of H_2 onto $\overline{R(K)}$, the closure of the range of K. Now, $Py \in R(K)$ if and only if

$$y = Py \ + \ (I - P)y \ \in \ R(K) + R(K)^{\perp} \ . \tag{8}$$

Therefore, a least squares solution exists if and only if y lies in the dense subspace $R(K) + R(K)^{\perp}$ of H_2. Now we have guaranteed the existence of a generalised solution for all y in a dense subspace of H_2. In taking up the issue of uniqueness, we note that (8) is equivalent to the condition $Kx - y \in R(K)^{\perp} = N(K^*)$, that is, $K^*Kx \ = \ K^*y$. Now we see that there is a unique least squares solution if and only if $\{0\} = N(K^*K) = N(K)$, and that the set of all least squares solutions is closed and convex. Therefore, there is a unique least squares solution of smallest norm which we call generalized solution. The mapping $K^{\dagger}$ that associates with a given $y \in D(K^{\dagger}) = R(K) + R(K)^{\perp}$ the generalized solution $K^{\dagger}y$ is called the Moore-Penrose generalized inverse of K. In our scheme $K^{\dagger}$ is then the mechanism which provides a unique solution for any $y \in D(K^{\dagger})$. In this sense, $K^{\dagger}$ settles the issues of existence and uniqueness for generalized solutions. In addition, we can give a convenient representation for $K^{\dagger}$ of compact linear operators K in terms of the singular system $\{v_j, u_j; \mu_j\}$. Indeed, if $y \in D(K^{\dagger})$, then $y = y_1 + y_2, y_1 \in R(K)$ and $y_2 \in R(K)^{\perp}$. Since $u_j \in R(K)$, we then have $< y, u_j >=< y_1, u_j >$ for all j and hence the vector

$$x \ = \ \sum_{j=1}^{\infty} \frac{< y_1, u_j >}{\mu_j} v_j \ = \ \sum_{j=1}^{\infty} \frac{< y, u_j >}{\mu_j} v_j \tag{9}$$

exists by Picard's criterion and satisfies $Kx = y_1$ and $x \in N(K)^{\perp}$. Thus x is a least squares solution lying in $N(K)^{\perp}$, that is,

$$K^{\dagger}y \ = \ \sum_{j=1}^{\infty} \frac{< y, u_j >}{\mu_j} v_j \ . \tag{10}$$

This representation of $K^{\dagger}y$ shows very clearly that $K^{\dagger}$ is unbounded if $R(K)$ is infinite dimensional. Indeed, a perturbation in y of the form δu_n gives a new right hand side of the form $y^{\delta} \ = \ y + \delta u_n$ satisfying $||y - y^{\delta}|| \ = \ \delta$. Yet the generalized solution satisfy

$$||K^{\dagger}y \ - \ K^{\dagger}y^{\delta}|| \ = \ \frac{\delta}{\mu_n} \quad \rightarrow \quad \infty \quad \text{as} \quad n \ \rightarrow \ \infty \ . \tag{11}$$

The big issue remains. Namely, in order for $Kx = y$ tobe well-posed it is necessary that $K^\dagger$ be continuous.

3.3. Regularization

The generalized Pseudoinverse operator $K^\dagger : D(K^\dagger) \rightarrow H_1$ is a closed densely defined linear operator which is bounded if and only if $R(K)$ is closed. But our operator K see equation (1) and (2), a Fredholm integral equation system of the first kind, is compact, then $R(K)$ is closed if and only if it is finite dimensional. But equations with square integrable kernels generate operators on L^2 which are compact and for not degenerated kernels $R(K)$ is infinite dimensional. That means $R(K)$ is open and so $K^\dagger$ is unbounded, i.e. $K^\dagger$ is discontinuous. The problem is ill-posed. If we wish to obtain a well-posed problem we need a so called regularization. In general regularizations are families of operators

$$K_\gamma : H_2 \rightarrow H_1 \quad \text{with} \quad \lim_{\gamma \rightarrow 0} K_\gamma y = K^\dagger y \quad \text{for all} \quad y \in D(K^\dagger) \ , \tag{12}$$

i.e. the convergence is pointwise on $D(K^\dagger)$, see Louis[4] . The parameter γ is the so called regularization parameter. In the case of noisy data y^δ with $||y - y^\delta|| \leq \delta$ we determine as solution

$$x_\gamma^\delta = K_\gamma \, y^\delta \ . \tag{13}$$

However, the total error consists of two parts

$$x_\gamma^\delta - x = K_\gamma(y^\delta - y) + (K_\gamma - K^\dagger)y \ . \tag{14}$$

The first part we call the data error and the second part the approximation error or regularization error. If $\gamma \rightarrow 0$ the approximation error tends to zero while the data error tends to infinity. Therefore, the total error can never be zero and we are in a dilemma. We have to look for an "optimal" regularization parameter γ which minimizes the total error.

4. PROJECTION METHODS AS REGULARIZATION

-

Our aim is now to approximate $K^\dagger y$. We know that, ignoring the trivial case in which the kernel $k(\cdot, \cdot)$ is degenerated, the generalized solution $K^\dagger y$ depends discontinuously on y, but we would like our approximation to depend continuously on y. There are a lot of regularization methods, we refer to Engl/Hanke/Neubauer.[5] The most popular and well-known is Tikhonov regularization. There are other examples like truncated singular value decomposition, see Louis,[4] iterative methods (e.g. linear Landweber iteration, see Hanke[6] or nonlinear conjugate gradient iteration, see Hanke[7] and Brakhage[8]), mollifier methods, see Louis/Maaß[9] and Böckmann/Biele/Neuber,[10] or maximum entropy methods, see Amato/Hughes.[11] But if one would like to solve a real practical problem the results of regularization from infinite dimensional spaces are unsuitable. Hence we need a discretization, see Engl.[12] We begin by considering two natural finite rank approximations to $K^\dagger$. On the one hand side it is possible to combine any regularization method with a projection method. On the other hand side we observe that pure projection into finite dimensional spaces act as regularization. Let $X_1 \subseteq X_2 \subseteq ... \subseteq H_1$ be finite dimensional subspaces of H_1 with $\overline{U_{n=1}^\infty} X_n = H_1$, i.e. dense in H_1, and $K_n := K_{|X_n}$ is the restriction of K to a subspace X_n of H_1. A natural way to generate a finite dimensional approximation is to find the minimal norm least squares solution of the equation $K_n x = y$. As an approximation of $K^\dagger y$ one could use the unique least squares solution, i.e. $K_n^\dagger y$ or $K_n^\dagger y^\delta$, respectively, where $||y - y^\delta|| \leq \delta$ represents the noise level of the data. The approximative solution $x_n \in X_n$ minimizes $||Kx - y^\delta||$ over X_n. Since X_n is finite dimensional, $R(K_n)$ is closed, i.e. $K_n^\dagger$ is continuous. The approximate problem is well-posed. We note the fact that in general $K_n^\dagger y$ does not converge for all $y \in D(K^\dagger)$, see Seidman.[13] Only with additional assumptions, we refer to Groetsch,[14] one can obtain convergence.

4.1. Convergence Assumptions

We need the uniform boundedness of the operators $\{R_n\}$ defined by $R_n := K_n^\dagger Q_n K$ where Q_n is the orthogonal projector of H_2 onto $K(X_n)$. Note that

$$R_n^2 = K_n^\dagger Q_n K_n K_n^\dagger Q_n K = K_n^\dagger Q_n Q_n Q_n K = R_n \tag{15}$$

hence R_n is a (generally nonorthogonal) projection operator.

LEMMA 41. *It holds* $K_n^\dagger y \rightarrow K^\dagger y$ *if* $n \rightarrow \infty$ *for each* $y \in D(K^\dagger)$ *if and only if* $\{||R_n||\}$ *is bounded.*

Proof. We prove only one direction. Note that

$$K_n^\dagger y = K_n^\dagger Q_n y = K_n^\dagger Q_n Q y = K_n Q_n K K^\dagger y = R_n K^\dagger y \tag{16}$$

where Q is the orthogonal projector of H_2 onto $\overline{R(K)}$. Suppose that $\{||R_n||\}$ is bounded and let $z_n \in X_n$ be the best approximation to $K^\dagger y$ in X_n. Since $N(K_n) = \{0\}$, we have

$$R_n z_n = K_n^\dagger Q_n K z_n = K_n^\dagger K_n z_n = z_n \tag{17}$$

and by (15)

$$\begin{aligned} ||K_n^\dagger y - K^\dagger y|| &\leq ||K_n^\dagger y - z_n|| + ||z_n - K^\dagger y|| \\ &= ||R_n z_n + R_n K^\dagger y|| + ||z_n - K^\dagger y|| \\ &\leq (||R_n|| + 1)||z_n - K^\dagger y|| \end{aligned}$$

tends to zero as $n \rightarrow \infty$. □

Supposed that $\{v_j, u_j; \mu_j\}$ is a singular system for K and that $X_n := \text{span}\{v_1, ..., v_n\}$. Then we observe

$$K_n^\dagger y = \sum_{j=1}^{n} \frac{1}{\mu_j} < y, u_j > v_j \quad , \tag{18}$$

i.e. $K_n^\dagger y$ is the truncated singular value decomposition and

$$\begin{aligned} R_n x &= K_n^\dagger \sum_{j=1}^{n} \mu_j < x, v_j > u_j \\ &= \sum_{j=1}^{n} \mu_j < x, v_j > K_n^\dagger u_j \\ &= \sum_{j=1}^{n} < x, v_j > v_j \quad . \end{aligned}$$

Therefore R_n is the orthogonal projector of H_1 onto X_n and hence $||R_n|| = 1$. In this case convergence occurs and

$$K_n^\dagger y \rightarrow \sum_{j=1}^{\infty} \frac{1}{\mu_j} < y, u_j > v_j = K^\dagger y \quad . \tag{19}$$

In addition, another more fortunately idea consists of a finite dimensional approximation over the range of K. Let $\{t_1, t_2, ...\} \subset \overline{R(K)}$ linear independent and the linear closure dense in $\overline{R(K)}$. We use as n-th approximation of $K^\dagger y$, $y \in D(K^\dagger)$, the solution x_n of the following problem: $< Kx, t_j > = < y, t_j >$, $j = 1, .., n$, $x \in X_n := \text{lin}\{K^* t_1, ..., K^* t_n\}$. The unique solution x_n can be determined as $x_n = \sum_{i=1}^{n} a_i K^* t_i$ where $a_1, ..., a_n$ are unknown and we have to solve the linear equation system

$$< y, t_j > = \sum_{i=1}^{n} a_i < K K^* t_i, t_j > = \sum_{i=1}^{n} a_i < K^* t_i, K^* t_j >, \; j = 1, .., n \quad . \tag{20}$$

It holds that x_n converge to $K^\dagger y$ for $n \rightarrow \infty$, see Engl.[12] In the case of noisy data we obtain

$$||x_n - x_n^\delta|| \leq \frac{\delta_n}{\sqrt{\rho_n}} \quad \text{with} \quad ||y_n^\delta - P_n y|| \leq \delta_n \tag{21}$$

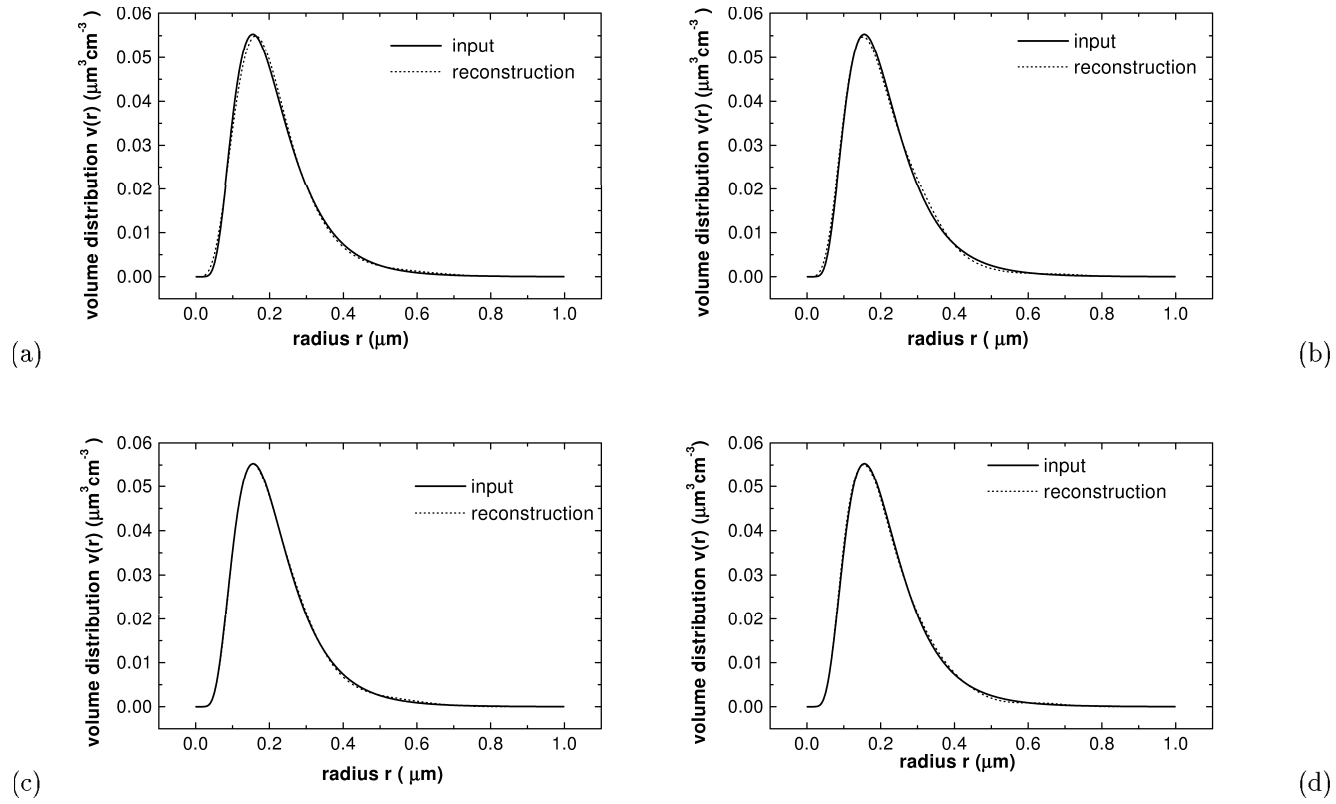

Figure 1. Reconstructions of the first example with 5+2 exact data, i.e. without 1064 nm, via different B-splines k=5, n=12 (a), k=6, n=19 (b), k=8, n=22 (c),k=9, n=26 (d).

and ρ_n is the smallest eigenvalue of the coefficient matrix of the system (20). Moreover, if $\delta_n \rightarrow 0$ and $\frac{\delta_n}{\sqrt{\rho_n}} \rightarrow 0$ with $n \rightarrow \infty$ then holds

$$\lim_{n \rightarrow \infty} ||x_n^\delta - K^\dagger y|| = 0 \quad . \tag{22}$$

In this case the value ρ_n acts as regularization parameter. The dimension n is allowed to grow only slowly on dependence of δ_n that (22) holds. Since in general $\lim_{n \rightarrow \infty} \rho_n = 0$ this is a restriction. Furthermore, according to the stability wishes of the data one has to choose the $\{t_n\}$ in that way that ρ_n is as large as possible. If K is compact as in our case with singular values $\{\mu_n\}$ it holds always with orthonormal $\{t_n\}$ $\rho_n \leq \mu_n^2$. Besides, if t_n are the singular vectors then $\rho_n = \mu_n^2$. The resulting method is again the truncated singular value decomposition which is in this sense "optimal" among the considered projection methods. Therefore, pure discretization turns out to be a regularization method. In addition, another possibility consists of a combination of a infinite dimensional regularization method, e.g. Tikhonov regularization or truncated singular value decomposition with projection. We call such a combination a hybrid method. In discretizing an ill-posed integral equation of the first kind an ill-conditioned linear equation system is produced. Generally, the finner the discretization, the closer the algebraic problem approximates the ill-posed continuous problem and hence the more ill-conditioned the algebraic problem becomes. In those hybrid methods the regularizing discretization and the additional regularization work hand-in-hand to produce an "optimal" linear equation system which coefficient matrix reflects the original ill-posed problem quite enough but is not high ill-conditioned.

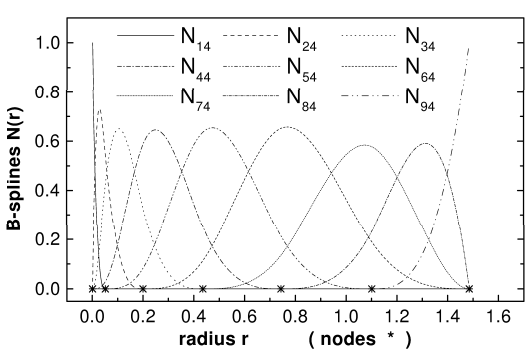

(a)

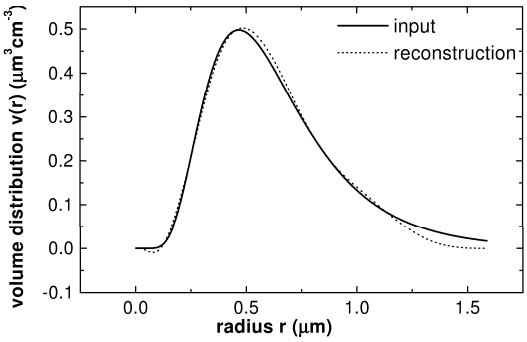

(b)

Figure 2. B-spline basis of dimension 9 and order 4 on a non-equidistant grid (a) and the reconstruction of the second example with 6+2 exact data (b).

5. HYBRID METHOD WITH VARIABLE PROJECTION

In this paper we propose a hybrid method, a combination of a variable projection method with truncated singular value decomposition. To turn into a finite dimensional problem we might simply try to solve the problem over a finite dimensional subspace of H_1. For example, if X_n is an n-dimensional subspace of H_1 spanned by the linearly independent vectors $\{w_1, ..., w_n\}$ then the vector $x^\delta_{n,\gamma}$ minimizes $||Kx - y^\delta||$ over X_n with a truncation level γ. The solution $x^\delta_{n,\gamma}$ can be represent as $x^\delta_{n,\gamma} = \sum_{j=1}^n d_i w_i$ where the unknown coefficients d_i, $i = 1, .., n$, are the generalized solution of the linear equation system

$$\sum_{i=1}^{n} \int_{r_{min}}^{r_{max}} k(r, \lambda_j) w_i(r) dr \; d_i \;=\; y(\lambda_j), \;\; j = 1, .., N + M, \tag{23}$$

which may be underdeterminate or overdeterminate, respectively. The points λ_j, $j = 1, .., N + M$, are the so called collocation points, in general the measurement points. We solve (23) with truncated singular value decomposition with level γ. We might call this type of discretization of a "finite element" discretization because the computed numbers d_i are coefficients of certain basis function $\{w_i\}$ which often will be taken as basic spline functions on some grid.

5.1. B-Spline Basis

Let $\Delta = \{r_0, ..., r_{l+1}\}$ a grid of $l + 2$ different nodes $r_{min} = r_0 < r_1 < ... < r_{l+1} = r_{max}$. A spline of degree $k - 1$ (order k) is a function $s \in C^{k-2}[r_{min}, r_{max}]$ which in every interval $[r_i, r_{i+1}]$, $(i = 0, .., l)$, consists of a polynom s_i with degree $\leq k - 1$. The spline space of degree $k - 1$ we denote by $S_{k,\Delta}$. We recognize that obviously the dimension is

$$\dim S_{k,\Delta} \;=\; k + l \;=: n \tag{24}$$

and that one common basis is

$$B := \{1, r, ..., r^{k-1}, (r - r_1)^{k-1}_+, ..., (r - r_l)^{k-1}_+\} \;\;, \tag{25}$$

see Deuflhard/Hohmann.[15] There are some disadvantages of that basis. First, the support of e.g. r^i is the complete $I\!R$, i.e. the support is not a local one. Second, if e.g. two nodes r_i and r_{i+1} are very closely packed then $(r - r_i)^{k-1}$ and $(r - r_{i+1})^{k-1}$ are "nearly" linear dependent. Therefore, the analysis of the splines

$$s(r) \;=\; \sum_{i=0}^{k-1} a_i r^i \;+\; \sum_{i=1}^{l} c_i (r - r_i)^{k-1}_+ \tag{26}$$

is an ill-conditioned problem with respect to noises of the coefficients c_i. A more advantageous basis we get with the recursion ($\chi_{[\tau_i,\tau_{i+1}]}$ denotes the characteristic function)

$$N_{i1}(r) := \chi_{[\tau_i,\tau_{i+1}]}(r) = \begin{cases} 1 & : \ r \in [\tau_i, \tau_{i+1}] \\ 0 & : \ \text{otherwise} \end{cases} , \tag{27}$$

$$N_{ik}(r) := \frac{r - \tau_i}{\tau_{i+k-1} - \tau_i} N_{i,k-1}(r) + \frac{\tau_{i+k} - r}{\tau_{i+k} - \tau_{i+1}} N_{i+1,k-1}(r) , \tag{28}$$

where $\tau_1 \leq ... \leq \tau_n$ are the extended nodes and $N_{ik}(r)$ are the B-splines of order k, $k = 1, .., n$ and $i = 1, ..., n-k$. Now the support $N_{ik} \subset [\tau_i, ..., \tau_{i+1}]$ is a local one, $N_{ik}(r) \geq 0$ for all $r \in \mathbb{R}$, $N_{ik}(r)$ is a piecewise polynom of degree $\leq k-1$ with respect to the interval $[\tau_j, \tau_{j+1}]$ and the N_{ik}, $i = 1, ..., n$ are local linear independent. Moreover, $B = \{N_{1k}, ..., N_{nk}\}$ is now a well-conditioned basis of $S_{k,\Delta}$, see Fig. 2 (a). It holds $1 = \sum_{i=1}^{n} N_{ik}(r)$ for all $r \in [r_{min}, r_{max}]$, i.e. the B-splines represent a positive decomposition of the unit. Each spline $s \in S_{k,\Delta}$ is a unique convex combination of the so called de Boor-points d_i of s with $s = \sum_{i=1}^{n} d_i N_{ik}$. Now our regularized solution has the description

$$x^{\delta}_{n,\gamma}(r) = \sum_{i=1}^{n=k+l} d_i \ N_{ik}(r) \tag{29}$$

and we have three regularization parameters k, n and γ. We establish the parameter γ, the truncation level only to be a fixed value of machine rounding. We direct our attention to the regularization parameters k and n in the next section.

6. APPLICATION OF VARIABLE PROJECTION METHOD

Equation (1) and (2) are formulated into a more specific form

$$y(\lambda_j) = \int_{r_{min}}^{r_{max}} \tilde{K^v}(r, \lambda; m) \ v(r) \ dr \tag{30}$$

with

$$\tilde{K^v}(r, \lambda_j; m) := \begin{cases} K^v_{\pi}(r, \lambda_j; m) & : \ \lambda_j \in \lambda^{\pi} \\ K^v_{ext}(r, \lambda_j; m) & : \ \lambda_j \in \lambda^{ext} \end{cases} , \tag{31}$$

where $y(\lambda_j)$ are the optical data, whether it is backscatter β or extinction α depending on λ_j with $\lambda^{\pi} = \{355, 400, 532, 710, 800, 1064[nm]\}$, i.e. $N = 6$ and $\lambda^{ext} = \{387, 607[nm]\}$, i.e. $M = 2$. The $v(r)$ term is the volume concentration distribution and

$$K^v_{\pi/ext}(r, \lambda; m) = \frac{3}{4r} Q_{\pi/ext}(r, \lambda; m) , \tag{32}$$

we refer to the equations (1), (2) and (3). The distribution $v(r)$ is approximated by a convex combination of B-splines of order k, see equation (29)

$$v(r) = \sum_{i=1}^{n=k+l} d_i \ N_{ik}(r). \tag{33}$$

Now we have two variable regularization parameters the order k and the number n of B-spline functions $N_{ik}, i = 1, ..., n$. However, there already algorithms exist with fixed number and fixed order, e.g. with order 1 (polynoms of degree 0) see Heintzenberg et al[20] and von Hoyningen-Huene/Wendisch[21] or with order 2 (polynoms of degree 1) see Qing et al[18] or Müller et al.[19] From a mathematical point of view it is more meaningful to use them variably as regularization parameters to obtain a well-conditioned (discrete) linear equation system, see (23). We call our algorithm a variable projection method.

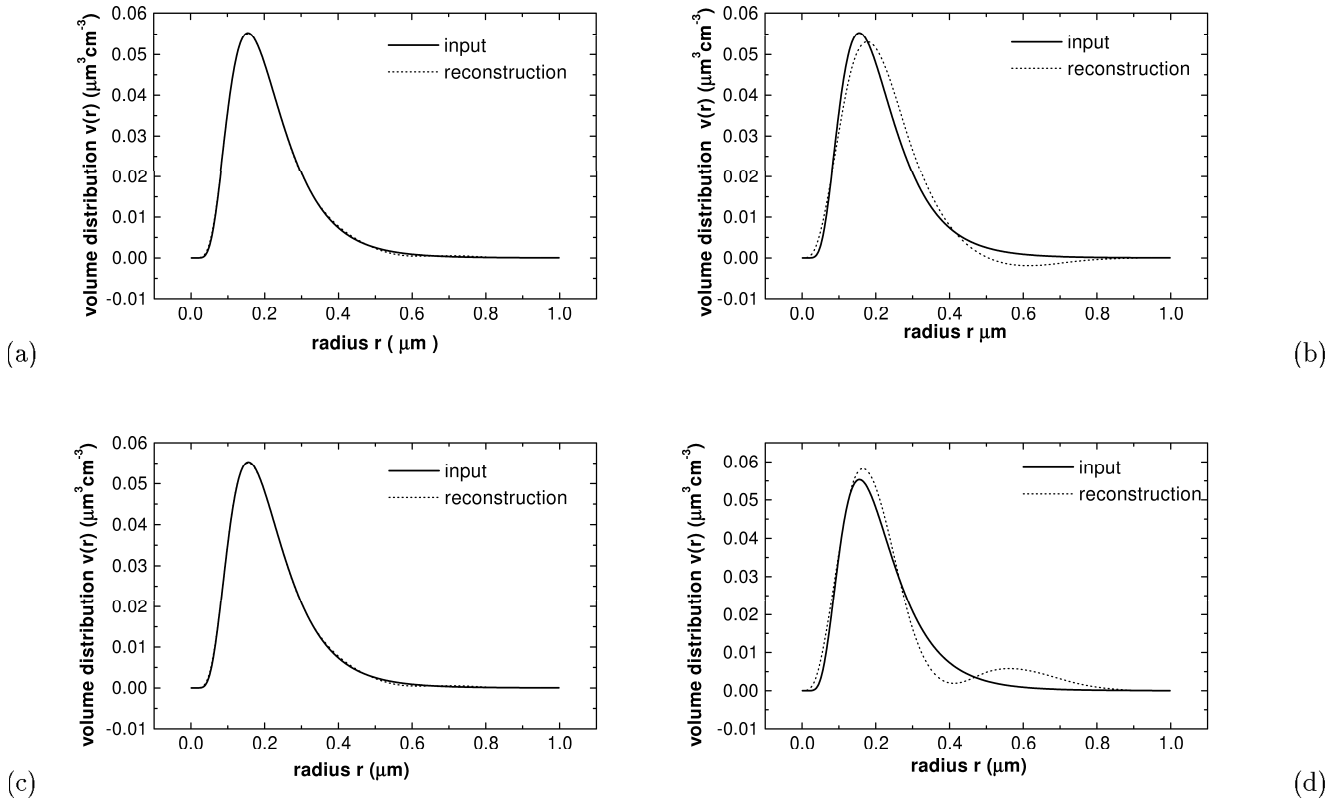

Figure 3. Results of the volume distribution for exact data with 6+2 (a) and with 5+2 (c) wavelengths, i.e. without 710 nm, and for noisy data (15 %) with 8 (b) and with 7 (d) wavelengths.

6.1. Numerical Results With Different B-splines

Logarithmic-normal distributions are used to describe the particle size distribution spectrum

$$n(r) \;=\; \frac{1}{r}\,\frac{1}{\sqrt{2\pi}\,\ln\sigma}\,\exp(-0.5\,\ln^2(\frac{\frac{r}{r_{med}}}{\ln\sigma}))\;. \tag{34}$$

The particle parameters of the first (second) example are $r_{med} = 0.1(0.3)\mu m$ and $\sigma = 1.6(1.6)$. Moreover, for the inversion we use the refractive index $m = 1.5 + 0.001i(1.475 + 0.005i)$ and the lower and upper integration limits $r_{min} = 0.001(0.001)\mu m$ and $r_{max} = 1.0(1.59)\mu m$. The hybrid method of variable projection presents excellent results for the first example at 7 wavelengths, see Fig. 1 , and for the second example at 8 wavelengths, see Fig. 2 (b). In the exact data case the inversion results are very excellent since the reconstructed distribution (dotted line) is more or less equal to the input distribution (solid line), see Fig. 1. Moreover, one can see that the inversion problem is not very sensible by variation of the order k if one use orders k in the range between 5 to 9 and dimensions n between 12 and 26, see Fig. 1 (a)-(d).

6.2. Experimental Setup

The lidar setup of the IfT consists of two Nd:YAG and two dye lasers emit pulses simultaneously at 355, 400, 532, 710, 800, and 1064 nm. The beams containing the six wavelengths are unified on a common optical axis and tenfold expanded. A flat scanning mirror permits one to align the lidar beam to arbitrary zenith angles. The elastically backscattered signals at the six wavelengths — at 532 nm with polarization discrimination — and the Raman signals

of nitrogen at 387 and 607 nm and of water vapor at 660 nm are measured. Profiles of the particle backscatter coefficients at the six emitted wavelengths, the particle extinction coefficient at 355 and 532 nm, the depolarization ratio at 532 nm, as well the as water-vapor mixing ratio are derived from the detected signals.

6.3. Numerical Results of Measurement Situations

For four different measurement situations we have made simulated inversions. The reconstruction results of the inversion from synthetic optical data were compared with the input distribution. The first measurement situation at 6+2 wavelengths (backscatter and extinction, respectively) is shown in Fig. 3 (a) for exact data and (b) for 15% Gaussian noise. The second situation at 5+2 wavelengths, without 710 nm, is shown in Fig. 3 (c) for exact data and (d) for 15% Gaussian noise. In the third situation we use only the measurements of the backscatter lidar at 6 wavelengths. The simulations with exact data (a) and for 10% Gaussian noise (b) are placed in Fig. 4. In the fourth situation we only take 3+1 simulated data at $\lambda^{\pi} = \{355, 532, 1064[nm]\}$, i.e. $N = 3$ and $\lambda^{ext} = \{532[nm]\}$, i.e. $M = 1$, see Fig. 4 (c) and (d). We observed that for exact data B-splines of order 5 (polynoms of degree 4) and $n = 19$ or $n = 12$ of B-splines (the dimension of the finite dimension reconstruction space) work very well in both of the first cases or in both of the last cases, respectively. This is plausible from a mathematical point of view since in both of the last cases we have not so much informations. Since a distribution function has to be zero at points r smaller then r_{min} and at points greater then r_{max} we propose to set $d_1 = 0$ and $d_n = 0$. If we test with noisy data, e.g. 15% Gaussian noise Fig. 3 (b), (d) or 10% Gaussian noise Fig. 4 (b), (d) we observed that the finite dimension has to be smaller again as in the exact cases, see Groetsch,[3] because the first part of equation (14) becomes greater if n increased. B-splines of order 4 (polynoms of degree 3) and of the dimension $n = 11$ show suitable reconstructions (dotted line). Fig. 3 (b), (d) shows that this reconstruction method provides excellent results up to 15% Gaussian noise in the first two measurement situations and up to 10% Gaussian noise in the last two situations, see Fig. 4 (b), (d). Besides, we used a non-equidistant grid. The left-hand roots of the Tschebyscheff polynoms were taken as nodes of the necessary grids, see Fig. 2 (a).

7. OUTLOOK

The refractive index of the particles is an unknown one in real measurement situations with a lidar setup only. We present some results in Fig. 5 which show that the inversion is not unique with respect to the refractive index. We reconstruct functions which have only positive values for all incorrect indices (couples of the black diagonal range in Fig. 5 (a) and (c)). One can not decide without additional information which function is the correct volume distribution.

Although there are some problems if the refractive index is unknown, the algorithm, however, shows that it is possible to provide excellent results for only 4 measurements up to 10%, noise, see Fig. 2 (d). For the unknown refractive index case we will install a nonlinear optimization method to reduce the black range. This improvement will be done next time.

ACKNOWLEDGMENTS

The authors would like to thank A. Ansmann, D. Müller and U. Wandinger from the Institute for Tropospheric Research in Leipzig for interesting discussions and for providing the multi-wavelength LIDAR measurements. They are grateful to A. Franke for his assistance during the computer tests. This work has been supported by the Bundesministerium für Bildung, Wissenschaft, Forschung und Technologie (BMBF) under grant 07AF310/2.

REFERENCES

1. A. Ansmann, U. Wandinger, M. Riebesell, C. Weitkamp and W. Michaelis, "Independent measurement of extinction and backscatter profiles in cirrus clouds by using a combined Raman elastic–backscatter lidar" *Applied Optics* **33**, pp. 7113-7131, 1992.
2. G. F. Bohren and D. R. Huffman, *Absorption and Scattering of Light by Small Particles*, John Wiley and Sons, New York, 1983.

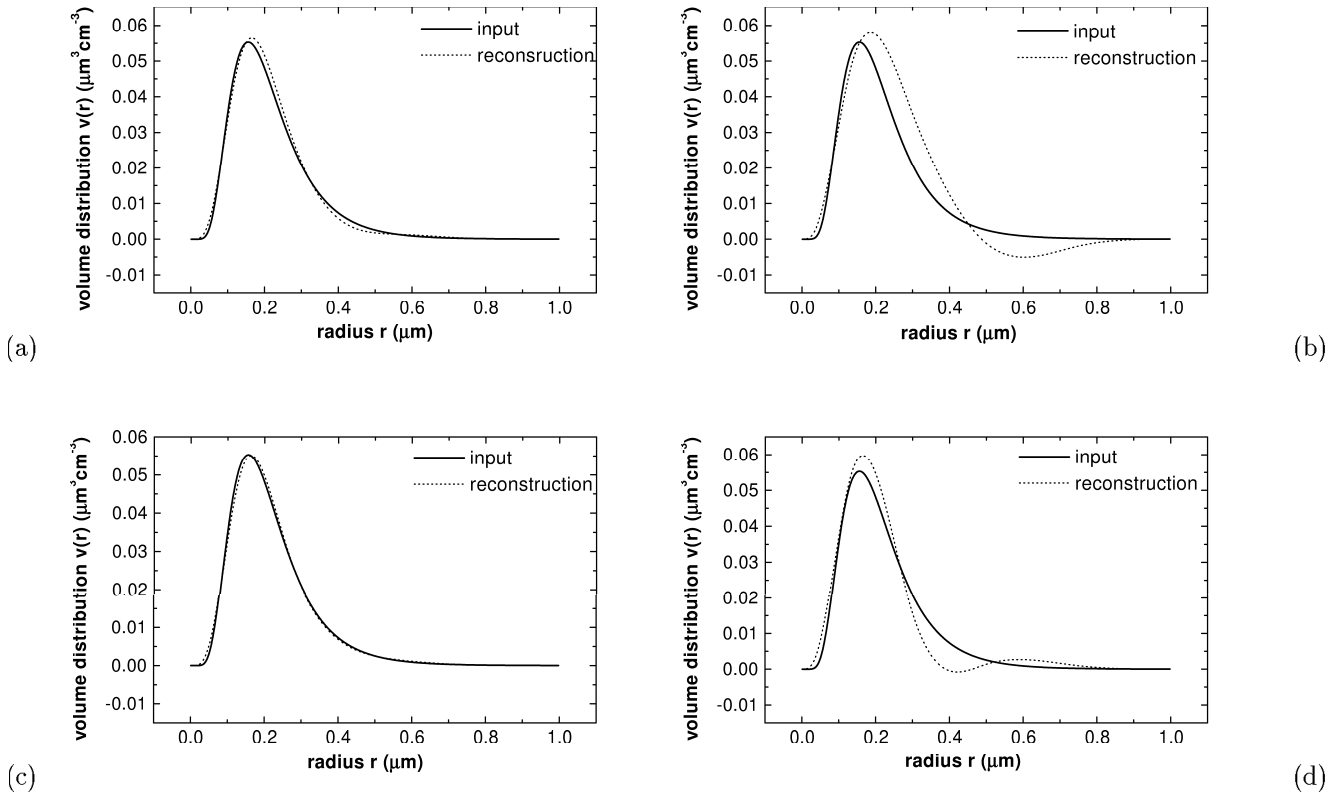

Figure 4. Results of the volume distribution for exact data with 6+0 (a) and with 3+1 (c) wavelengths and for noisy data (10 %) with 6 (b) and with 4 (d) wavelengths.

3. C. W. Groetsch, *Inverse Problems in the Mathematical Sciences*, Vieweg und Sohn, Braunschweig, Wiesbaden, 1993.
4. A. K. Louis, *Inverse und schlecht gestellte Probleme*, B.G. Teubner, Stuttgart, 1989.
5. H. W. Engl, M. Hanke and A. Neubauer, *Regularisation of Inverse Problems*, Kluwer Academic Publishers, Dordrecht, Boston and London, 1996.
6. M. Hanke, "Accelerated Landweber iterations for the solution of ill-posed equations", *Numerische Mathematik* **60**, pp. 341-373, 1991.
7. M. Hanke, *Conjugate Gradient Type Methods for Ill-posed Problems*, Longman Scientific & Technical, Harlow Essex, 1995.
8. H. Brakhage, "On ill-posed problems and the method of conjugate gradients", *Inverse and Ill-posed problems*, eds H. W. Engl and C. W. Groetsch, Academic Press, Boston, 1986.
9. A. K. Louis and P. Maaß, "A Mollifier Method for Linear Operator Equations of the First Kind" *Inverse Problems* **6**, pp. 427-440, 1990.
10. C. Böckmann, J. Biele and R. Neuber, "Analysis of multi-wavelength lidar data by inversion with mollifier method", *Pure Appl. Opt.* **7**, pp. 827-836, 1998.
11. U. Amato and W. Hughes, "Maximum entropy regularization of Fredholm integralequations of the first kind " *Inverse Problems* **7**, pp. 793-808, 1991.
12. H. W. Engl, *Integralgleichungen*, Springer, Wien, New York, 1997.
13. T. I. Seidman, "Nonconvergence results for the application of least squares estimation to ill-posed problems", *J. Optimiz. Th. Appl.* **30**, pp. 535-547, 1980.

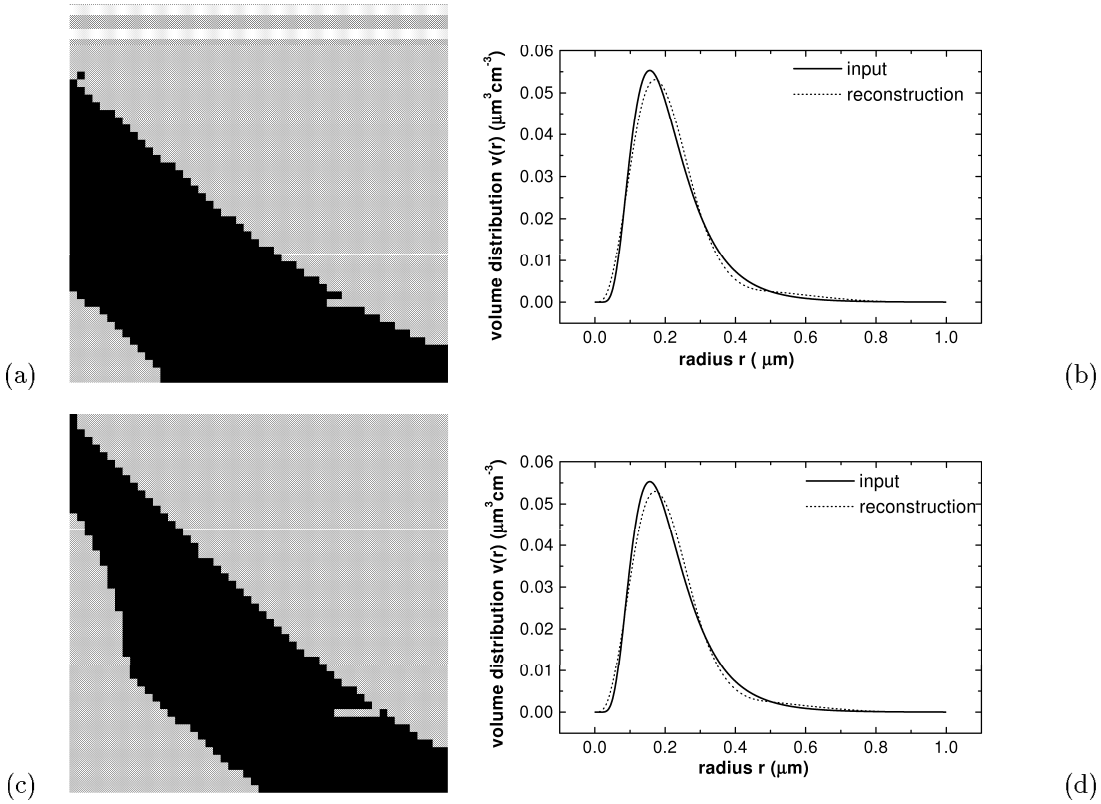

Figure 5. The refractive indices (imaginary part: 0-0.05 horizontal; real part: 1.4-1.6 vertical; smallest values at the top left) with resulting positive (level 0.001) distributions (black) (a), (c) and reconstruction results for the volume distribution function for the exact refractive indices m=1.5+0i (b), for m=1.5+0.01i (d).

14. C. W. Groetsch, *The theory of Tikhonov regularization for Fredholm equations of the first kind*, Pitma Publishing, Boston, London, Melbourne, 1984.
15. P. Deuflhard and A. Hohmann, *Numerische Mathematik*, de Gruyter, Berlin, New York, 1991.
16. C. Böckmann, "Projection Method for Lidar Measurements", *Advanced Mathematical Tools in Metrology III*, eds P. Ciarlini, et al, World Scientific, Singapore, pp. 239-240, 1997.
17. C. Böckmann and J. Niebsch, "Mollifier Methods for Aerosol Size Distribution" *Advances in Atmospheric Remote Sensing with Lidar*, eds A Ansmann, et al, Springer, New York, Berlin, Heidelberg, pp. 67-70, 1996.
18. P. Qing, H. Nakane, Y. Sasano and S. Kitamura, "Numerical simulation of the retrieval of aerosol size distribution from multiwavelength laser radar measurements", *Applied Optics* **28**, pp. 5259-5265 , 1989.
19. D. Müller, U. Wandinger and A. Ansmann, "Microphysical particle parameters from extinction and backscatter lidar data by inversion through regularization: Theory", *Applied Optics* **38**, to appear 1999.
20. J. Heintzenberg, H. Müller, H. Quenzel and E. Thomalla, "Information content of optical data with respect to aerosol properties: numerical studies with a randomized minimization-search-technique inversion algorithm" *Applied Optics* **20**, pp. 1308-1315, 1981.
21. W. von Hoyningen-Huene and M. Wendisch, "Variability of aerosol optical parameters by advective processes", *Atmos. Environ.* **28**, pp. 923-933, 1994.